Microchimica Acta
https://doi.org/10.1007/s00604-018-2790-x

ORIGINAL PAPER

Electrochemiluminescence based competitive immunoassay for Sudan I by using gold-functionalized graphitic carbon nitride and Au/Cu alloy nanoflowers

Wanlu Chen[1] · Xun Yao[2] · Xinchun Zhou[1] · Kang Zhao[1] · Anping Deng[1] · Jianguo Li[1]

Received: 25 February 2018 / Accepted: 3 April 2018

Abstract

A flower-like Au/Cu alloy nanocomposite (Au/Cu NFs) was synthesized and used in an electrochemiluminescence (ECL) based method for sensitive determination of the dye Sudan I. The Au-g-C_3N_4 nanosheets as an ECL emitter were prepared by electrostatic adsorption between gold nanoparticles and g-C_3N_4. They form a film on a glassy carbon electrode (GCE) and then can be connected with Sudan I antigen via gold-nitrogen bond and amidation reactions. The Au/Cu NFs combined with Sudan I antibody also via the Au-N bond and was introduced into the modified GCE by specific recognition between the antibody and the antigen. The overlap between emission spectra of the Au-g-C_3N_4 nanosheets and absorption spectra of Au/Cu NFs enabled the appearance of ECL resonance energy transfer process. That is, when the Sudan I analyte not present, the ECL was weakened due to absorption by the gray Au/Cu NFs on applying voltages from −1.7 V to 0 V. Conversely, the Au/Cu NFs on the GCE are reduced due to the competition for the antibody between the analyte and the antigen. A strong green ECL emission was obtained. The ECL response is linear in the 0.5 pg mL^{-1} to 100 ng mL^{-1} Sudan I concentration range, and the detection limit is 0.17 pg mL^{-1}.

Keywords Competitive immunosensor · Biosensor · ECL resonance energy transfer · Sudan dyes · Au/Cu nanocomposites

Introduction

Sudan I [1-(phenylazo)-2-naphthol] belongs to a kind of lipophilic azo compounds in the class of azo dyes including Sudan II, Sudan III, Sudan IV, Sudan Red B etc. It has been used to improve the luster of commercial products [1]. Since pharmacological studies have shown that Sudan I has certain toxicity and carcinogenicity, the European Union (EU) and other countries including China have banned it as a pigment added to the food [2–4]. However, they are still illegally utilized to advance the beauty of foodstuffs such as chili sauce and chilli powder [5–7]. Therefore, the control of Sudan I in food products is very crucial and the development of a rapid and economic detection method is urgently needed. In spite of the conventional measurement techniques for Sudan I are accurate and reliable such as liquid chromatography [8] and fluorescence assay [9], these methods need expensive instruments, complex pre-treatment steps and long time-consuming procedures. Remarkably, electrochemi-luminescence (ECL), combining the electrochemistry and chemiluminescence analysis, has already attracted extensive attentions due to its high sensitivity detection, simplified optical setup and low background noise [10–13].

Graphite-like carbon nitride nanosheets (g-C_3N_4 NHs) are a kind of metal-free semiconductor nanomaterials with stable s-triazine ring structure. Simultaneously, it is regarded as the most stable allotrope of carbon nitride at ambient conditions. As a novel ECL luminophore, g-C_3N_4 NHs presents charming

Electronic supplementary material The online version of this article (https://doi.org/10.1007/s00604-018-2790-x) contains supplementary material, which is available to authorized users.

✉ Anping Deng
denganping@suda.edu.cn

✉ Jianguo Li
lijgsd@suda.edu.cn

[1] The Key Lab of Health Chemistry & Molecular Diagnosis of Suzhou, College of Chemistry, Chemical Engineering & Materials Science, Soochow University, Suzhou 215123, China

[2] Zhangjiagang Entry-Exit Inspection & Quarantine Bureau, Zhangjiagang 215600, People's Republic of China

Published online: 01 May 2018

advantages and has been widely used in ECL sensors for sensitive determination of cholesterol [14], concanavalin A [15], metal ions [16], dopamine [17] and rutin [18]. Nevertheless, the ECL reaction will be blocked on account of a poor conductive layer caused by partial electro-reduction when the injection of highly energetic electrons into the conduction bands of g-C_3N_4 [19]. For improving the ECL properties of g-C_3N_4, it has been appropriately functionalized with some nanomaterials such as Ag [20], Pd [21] and carbon nanotubes [22]. Chen's group [23] found that excellent analytical performances are obtained when gold nanoparticles (Au NPs) was decorated on g-C_3N_4 because of its good biocompatibility and electrical conductivity. Despite the superior performance of this nanocomposite, it has been rarely reported in competitive electrochemical immunoassays based on ECL resonance energy transfer (ECL-RET).

ECL-RET have been a promising strategy for the design of immunosensor with high sensitivity and excellent accuracy [24, 25], which occurs when the donor's ECL spectrum has an appropriate overlap with the acceptor's absorption spectrum. To meet the requirement, the selection of a suitable pair of acceptor and donor is vital. Notably, metal nanocrystals exhibit splendid physical and chemical properties [26–28], which are produced by mixing two or more species such as hybrid, core-shell or alloy structures. Au/Cu alloy with a gorgeous biocompatibility has been found that its absorption spectra well matched with the ECL spectra of g-C_3N_4, which enabled the ECL-RET between g-C_3N_4 and Au/Cu flower-like nanocrystals (Au/Cu NFs). After some improvements, the Au/Cu NFs in this work has a larger specific surface area and more uniform structure compared with the earlier reported ones, indicating that there will be more binding sites for the antibody and more stable quenching performance.

A versatile competitive ECL immunosensor based on ECL-RET has been developed for measurement of Sudan I using Au/Cu NFs and Au-g-C_3N_4 nanosheets (Au-g-C_3N_4 NHs) as the acceptor and donor, respectively. Au NPs as an enhancer was chemically decorated onto the surface of g-C_3N_4 to form effective luminophore. And the ECL was weakened due to absorption by the gray Au/Cu NFs. The biosensor manifested remarkable sensitivity, reproducibility and precision, which results from the significant quenching effect and simple assembly process, indicating that the competitive ECL immunosensor provides an effective strategy for ultrasensitive detection of Sudan I and other small molecules.

Experimental

Materials

Melamine (2,4,6-triamino-1,3,5-trazine, 95%) was purchased from Beijing InnoChem Science & Technology Co., Ltd. (www.inno-chem.com.cn). Chloroauric acid ($HAuCl_4 \cdot 4H_2O$, 47.8%) and ethyl alcohol (99.7%) were acquired from Sinopharm Chemical Reagent Co., Ltd. (China, www.sinoreagent.com). Nitric acid (HNO_3, 65–68%) was provided from Chinasun Specialty Products Co., Ltd. (China, www.qschem.com/index.html). Cupric chloride dehydrate ($CuCl_2 \cdot 2H_2O$, 99.99%), Sudan III, Sudan IV and Lemon Yellow were bought from Aladdin Industry Corporation (www.aladdin-e.com/zh_cn). Sudan II, Bright Blue and Sunset Yellow were obtained from Macklin (China, www.macklin.cn). Ethyl-3-(dimethyl aminopropyl) carbodiimide (EDC, 98%) and N-hydroxysuccinimide (NHS, 97%) were supplied by J&K Scientific (China, www.jkchemical.com). Sudan I, Hexadecylamine (HAD, 90%), Bovine serum albumin (BSA, 98%) and ovalbumin (OVA) were acquired from Sigma-Aldrich Co., Ltd. (USA, www.sigmaaldrich. com/united-states. html). Dimethylformamide (DMF) was purchased from Amresco (https://www.amresco-inc.com). N,N-dicyclohexylcarbodiimide (DCC) was obtained from Fluka (USA, www.sigmaaldrich. com/united-states. html). Aluminum oxide polishing powder (Al_2O_3, 1.0, 0.3 and 0.05 μm) was obtained from Tianjin Aidahengsheng Technology Co., Ltd. (China, www.tjaida.cn). The polyclonal Ab against Sudan I and coating antigen (Sudan I-OVA) were prepared by our group and evaluated by ELISA. The detailed synthesis steps are given in the Electronic Supporting Material (ESM).

0.1 M pH 7.4 phosphate buffer saline (PBS) containing of NaCl (100 mM), Na_2HPO_4 (6.4 mM) and KH_2PO_4 (1.0 mM) were used as a washing buffer. ECL detection buffer was prepared by 0.1 M $K_2S_2O_8$-PBS. All other reagents and chemicals were commercially available and of analytical reagent grade. All aqueous solutions were prepared with sub-boiling doubly distilled water.

Apparatus

The ECL emissions were recorded by using a MPI-A multifunctional electrochemical analytical system (Xi'An Remax Electronic Science & Technology Co. Ltd., Xi'An, China, www.chinaremex.com) in the ECL detection buffer, and the working potential was 0 ~ −1.7 V with the voltage of the photomuitplier tube (PMT) (detection range from 300 to 800 nm) set at −500 V. The experiment applied a conventional three-electrode system which was composed of a modified glass carbon working electrode (GCE, φ = 3 mm), an Ag/AgCl reference electrode (KCl saturated) and a Pt wire counter electrode.

UV-vis absorption spectrum was recorded with Agilent 8453 UV-vis spectrophotometer (Agilent Co., America, www.chem.agilent.com). Electrochemical impedance spectroscopy (EIS) was carried out on a RST electrochemical working station (Suzhou Risetest Instrument Co., Ltd., China,

www.rst9999.com). The Scanning Electronic Microscopy (SEM) was supplied by Hitachi SU8010 SEM (Hitachi Co., Japan, www. hitachi. com). The Transmission Electron Microscope (TEM) images were obtained from Tecnai G2 F20 S-TWIN 200KV (FEG, FEI Co., USA). X-ray photoelectron spectroscopy (XPS) was performed on an ESCALab220i-XL electron spectroscopy from VG Scientific.

Preparation of Au-g-C_3N_4 NHs

The bulk g-C_3N_4 was synthesized by direct pyrolysis of melamine following a slightly modified literature procedure [19]. As shown in Scheme 1b, 10 mg of g-C_3N_4 NHs was dispersed into 10 mL of gold colloidal solution (synthesized by sodium citrate reduction of $HAuCl_4$ in aqueous solution) with gently stirring at room temperature for 24 h. Subsequently, the mixture was centrifuged to remove excess unbound gold nanoparticles. The light purple product was Au-g-C_3N_4 nanosheets (Au-g-C_3N_4 NHs) and stored at 4 °C for further use.

Synthesis of Ab/Au/Cu

Au/Cu NFs were synthesized as follows: 225 mg of HDA was dissolved in 20 mL of ultrapure water adequately, followed by adding 1.5 mL 100 mM $HAuCl_4{\cdot}4H_2O$ and $CuCl_2{\cdot}2H_2O$, respectively. Subsequently, 1.4 mL of glucose aqueous (1 M) was dropwise added into the above solution. After stirring for 12 h at room temperature, the mixture was transferred into oil bath, and then heated at 100 °C for 30 min under magnetic stirring. Finally, the nanocrystals were centrifuged to remove excess precursor and dried.

10 μL of Sudan I antibody was added into Au/Cu NFs aqueous solution (1 mg mL^{-1}) and incubated for 12 h at 4 °C. Then, antibody (Ab) was immobilized on the surface of Au/Cu NFs via Au-N bond. Finally, 10 μL of BSA (5%) was pipetted to the incubative solution for 1 h. The extra precursor was removed by centrifugation. The Ab/Au/Cu was dispersed in PBS and stored at 4 °C. The procedure for synthesis of Ab/Au/Cu is shown schematically in Scheme 1a.

Assembly of the immunosensor

Initially, the glassy carbon electrode (GCE, Φ = 3 mm) was burnished on a chamois sufficiently with α-Al_2O_3 powder to a mirror-like, and then thoroughly rinsed with ethanol and ultrapure water, allowed to dry with N_2 at room temperature. Thereafter, 10 μL of the Au-g-C_3N_4 NHs suspension was dropped onto the pretreated GCE and dried in air. The Au-g-C_3N_4/GCE was then incubated with Sudan I coating antigen (Ag) at 4 °C overnight to anchor the Ag through the Au-N bond and the amide reaction. Finally, 10 μL of BSA (5%) was pipetted to the modified GCE surface to block remaining active sites and eliminate nonspecific adsorptions for 1 h. After being rinsed with PBS and dried with N_2, the ECL biosensor was stored at 4 °C. The procedure for constructing the biosensor is shown schematically in Scheme 1.

Detection of Sudan I with electrochemiluminescence

Competitive immunoassay method was chosen for quantifying Sudan I, where Sudan I analyte competed with

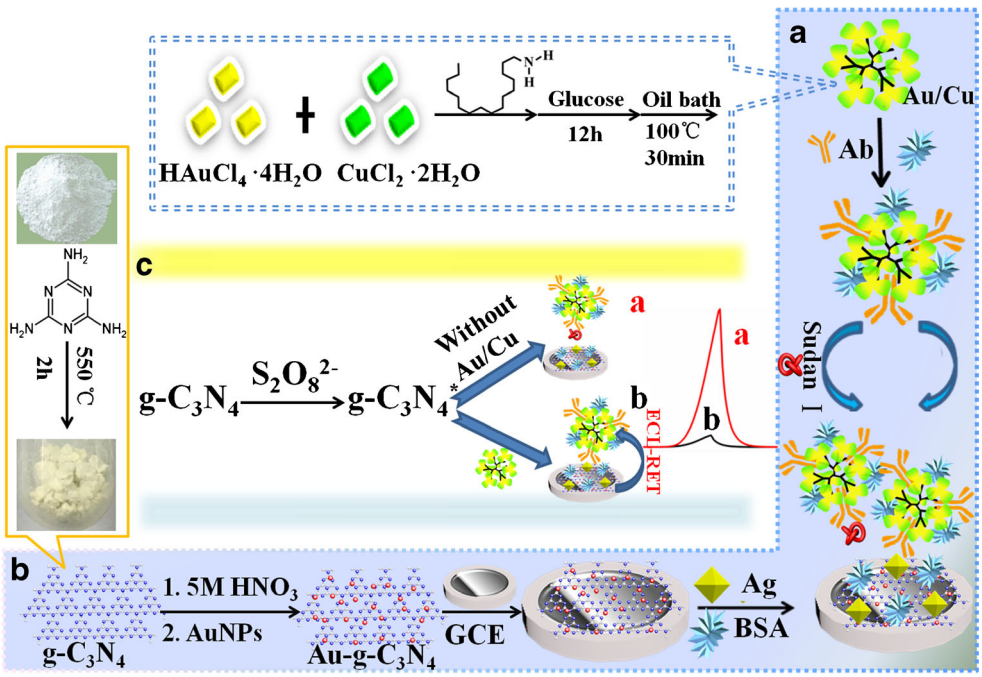

Scheme 1 Schematic illustration of (a) Synthesis Process of Au/Cu NFs labeled antibody ECL probe, (b) the fabrication of the biosensor, and (c) the ECL reaction mechanism

antigen for the certain amount of antibody. That is, the same 10 μL Ab/Au/Cu bioconjugate was first added into the 10 μL of different concentrations of Sudan I analyte. Then, the above mixture was coated on the biosensor for 1 h, followed by washing with PBS. Both the antigen on the biosensor and the analyte can combine with the antibody. There is the more Sudan I analyte, the fewer Ab/Au/Cu that can combine with the antigen. The Ab/Au/Cu and analyte that are not bound to the antigen are washed away by PBS. Eventually, the fabricated GCE was scanned in ECL detection buffer, and the ECL signal would change relative to the concentration of Sudan I standard solution, which was applied as the quantitative criterion of Sudan I. When the Sudan I analyte not presented, the ECL was weakened due to absorption by the gray Au/Cu NFs (Scheme 1c), cruve b). Conversely, the Au/Cu NFs on the GCE was reduced due to the competition for the antibody between the analyte and the antigen. A strong green ECL emission was obtained (Scheme 1c, cruve a).

Preparation of real-life samples

To test the practical application of the biosensor, three food samples (chili sauce, chili powder and tomato sauce) were purchased from a local supermarket in Suzhou (China) for spiking experiments. Briefly, 1 mL of different concentrations of Sudan I methanol solution (10 ng mL^{-1}, 1 μg mL^{-1} and 100 μg mL^{-1}) was added into the centrifuge tube, which 1 g of sample was weighed into. The spiked samples were vigorously shaken for 20 min and kept at 4 °C overnight. Then, 9 mL of MeOH was added into the tube. The extraction was performed by sonication for 20 min, followed by centrifugation at 12000 rpm for 6 min. The supernatant was diluted with water at 1:99 [5]. Theoretically, the final Sudan I concentration in all diluted samples were at 0.001, 1 and 100 ng mL^{-1}. Unspiked sample diluted with the same times was used as blank.

Results and discussion

Characterization of different nanomaterials

TEM image provides the feature of the g-C_3N_4 NHs and Au-g-C_3N_4 NHs, which distinctly indicates that g-C_3N_4 NHs possesses two-dimensional sheet-like structures (Fig. 1a) and a large number of black dots (~16 nm) corresponding to the Au NPs are homogeneously dispersed on the g-C_3N_4 NHs surfaces (Fig. 1b). The inset also illustrates that the suspension turns from nearly transparent g-C_3N_4 NHs to purple after the decoration of Au NPs. The well distributed of Au NPs on the surfaces of g-C_3N_4 NHs may arise from the electrostatic interactions between the positively charged g-C_3N_4 NHs and the negatively charged AuNPs and the co-action of the Au-N bond. FT-IR spectra and XPS spectra are used to further support the successful synthesis of Au-g-C_3N_4 NHs and exhibits in Fig. S1 (ESM).

Scanning electron microscopy (SEM) is firstly utilized to characterize the size and morphology of the Au/Cu NFs. Figure 1c shows the Au/Cu NFs displayed a spiny flower structure with an average size about 250 nm, which provides more uniform structure and a large specific surface area for attaching antibody compared with previous works. To further demonstrate the successful synthesis of the Au/Cu NFs, X-ray photoelectron spectroscopy (XPS) is used to investigate the elemental components. The results are shown in Fig. S2.

EIS characterization of immunosensor

Electrochemical impedance spectroscopy (EIS) is an effective method for making sure whether the process of electrode modification was successful or not. The EIS Nyquist plots in Fig. 2a consist of two parts: the linear portion and the semicircle section, which the former corresponds to the diffusion process at low frequencies, and the latter represents the electron-transfer resistance (Ret) at high frequencies. The Ret indicates the restricted diffusion of the substance modified on the surface of GCE. Compared with bare GCE (curve c), the g-C_3N_4 modified electrode exhibits a really small Ret

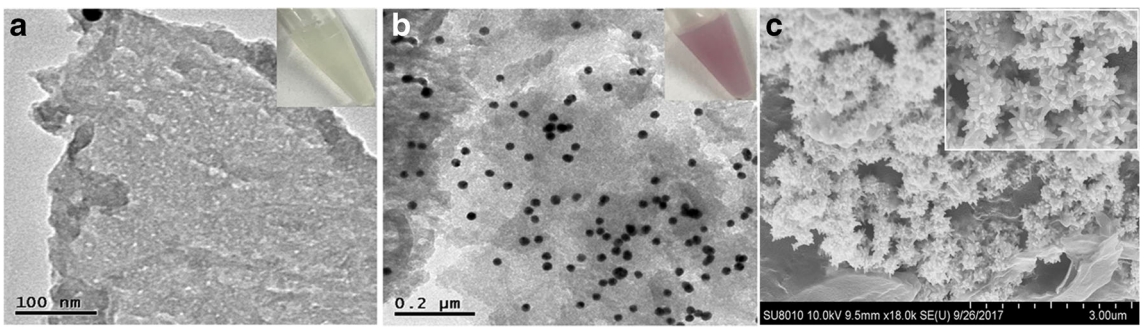

Fig. 1 **a** TEM image of g-C_3N_4 NHs and (**b**) Au-g-C_3N_4 NHs. **c** SEM image of Au/Cu NFs

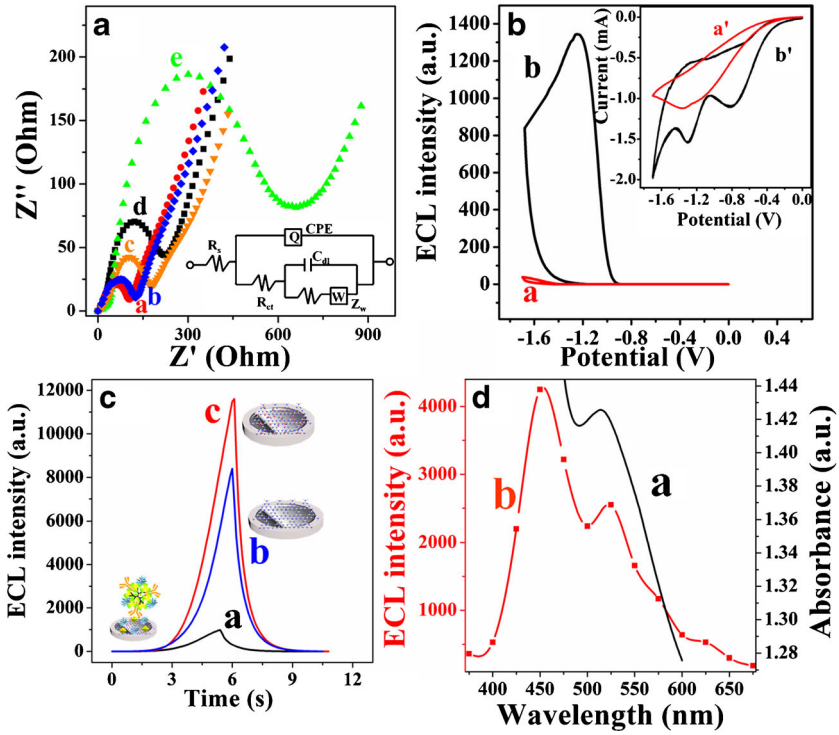

Fig. 2 **a** EIS of (a) GCE/Au-g-C_3N_4, (b) GCE/g-C_3N_4, (c) bare glassy carbon electrode (GCE), (d) GCE/Au-g-C_3N_4/Ag and (e) GCE/Au-g-C_3N_4/Ag/BSA in 0.1 mol L^{-1} KCl solution containing 5 mmol L^{-1} $[Fe(CN)_6]^{3-/4-}$ (Bottom inset: The equivalent circuit.). **b** ECL curve and cyclic voltammogram (inset) of the detection Sudan I in 0.1 M PBS containing (a) only 0.1 M KCl, (b) 0.1 M KCl and 0.1 M $K_2S_2O_8$. **c** ECL intensity of immunosensor (a) GCE/Au-g-C_3N_4/Ag/Ab/Au/Cu, (b) GCE/g-C_3N_4/Ag and (c) GCE/Au-g-C_3N_4/Ag. (D) UV-vis absorption spectrum of Au/Cu NFs (a), ECL spectrum of the Au-g-C_3N_4 NHs modified GCE (b) obtained by a series of optical filters (from 375 nm to 675 nm, spaced 25 nm)

(curve b). It worth noting that the Ret further decreases when Au-g-C_3N_4 was modified on the electrode as shown in curve a, proves that the Au NPs possess excellent electric conductivity. The resistance increases accordingly when the electrodes are modified by Au-g-C_3N_4-Ag (curve d), Au-g-C_3N_4-Ag-BSA (curve e). The reasons for the resistance increasing are that poor conductive properties of biomacromolecules obstruct mass transport and electron transfer of the modified GCE and solution. The Randle's equivalent circuit (the bottom inset of Fig. 2a) has been designed for better understanding the interfaces between solution and electrode, in which Rs, Cdl, CPE and Zw refer to the ohmic resistance, the double layer capacitance, constant phase element and the Warburg impedance, respectively. Therefore, EIS results demonstrate that the immunosensor was successfully fabricated.

Electrochemical and ECL behavior of immunosensor

In order to ascertaining the possible reaction mechanism of g-C_3N_4 NHs and $S_2O_8^{2-}$, cyclic voltammograms (CVs) and ECL-potential curves of g-C_3N_4 NHs in PBS (buffered saline) containing 0.1 M $S_2O_8^{2-}$ were studied and presented in Fig. 2b. The inset indicates that compared with the curve a', which without $K_2S_2O_8$, a reduction peaks of $K_2S_2O_8$ at −0.78 V is observed in the curve b' when the $S_2O_8^{2-}$ was added to PBS solution. Accordingly, the ECL signal is obviously generated after the modification of g-C_3N_4 NHs with $K_2S_2O_8$ (curve b). Thus, it is in conclusion that the ECL response of g-C_3N_4 NHs mainly arises from the reaction between g-C_3N_4 NHs and $K_2S_2O_8$. Based on the above experimental results and the previous reports [29, 30], the possible ECL processes is expressed in ESM.

As shown in Fig. 2c (curve b and c), the employment of Au NPs is beneficial to enhance the ECL emission of g-C_3N_4

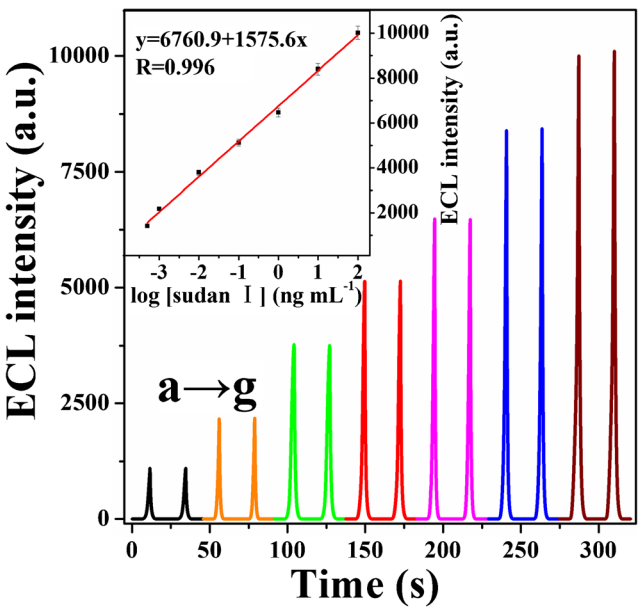

Fig. 3 Cyclic ECL curves of GCE/Au-g-C_3N_4/Ag/Ab/Au/Cu for Sudan I detection at (a) 0.0005 ng mL^{-1}, (b) 0.001 ng mL^{-1}, (c) 0.01 ng mL^{-1}, (d) 0.1 ng mL^{-1}, (e) 1 ng mL^{-1}, (f) 10 ng mL^{-1} and (g) 100 ng mL^{-1}. Inset: linear calibration plot for Sudan I detection ($n = 3$)

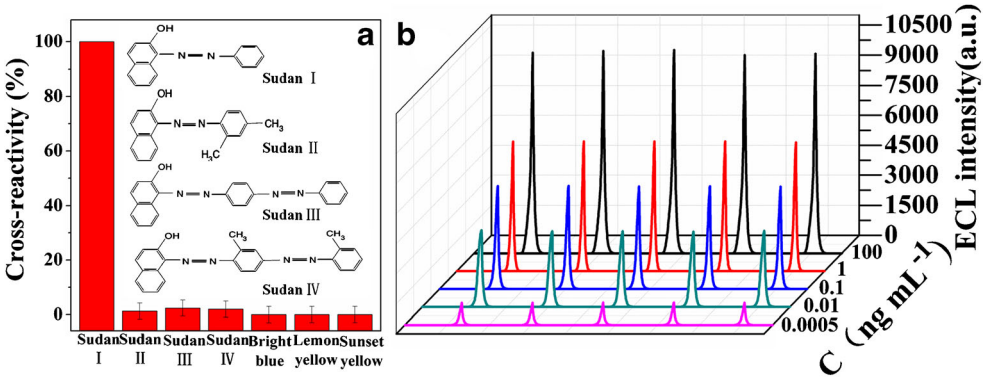

Fig. 4 **a** Selectivity of the biosensor for Sudan I determination over other interferences. **b** Continuous cyclic scans of immunosensor formed at 100 ng mL^{-1}, 1 ng mL^{-1}, 0.1 ng mL^{-1}, 0.01 ng mL^{-1} and 0.0005 ng mL^{-1} Sudan I standard solutions, respectively

NHs. The reason may be the excellent electric conductivity of Au NPs that can accelerate electron transfer rate on the surface of modified GCE. However, the ECL intensity of Au-g-C_3N_4 NHs (curve a) is remarkably quenched once Au/Cu NFs is subsequently brought to the electrode. For purpose of further demonstrating the quenching mechanism between Au/Cu NFs and Au-g-C_3N_4 NHs, some experiments were conducted and rendered in Fig. 2d. As displayed in curve a, the typical UV-vis absorption range of Au/Cu NFs is 500–600 nm, while the ECL emission range of Au-g-C_3N_4 NHs is about 400–650 nm (curve b) [31]. The overlap between emission spectra of the Au-g-C_3N_4 NHs (donor) and absorption spectra of Au/Cu NFs (acceptor) enable the appearance of RET process, which can quench the ECL intensity of Au-g-C_3N_4 NHs.

Optimization of immunoreaction conditions

In order to obtain the optimal condition, the following parameters were optimized: (a) volume of Au/Cu NFs; (b) concentration of Au-g-C_3N_4 NHs; (c) concentration of antigen; (d) concentration of antibody. Respective data and Figures are given in the ESM. The following experimental conditions were found to give best results: (a) Best volume of Au/Cu NFs: 80 μL; (b) Optimal concentration of Au-g-C_3N_4 NHs: 0.5 mg mL^{-1}; (c) Optimal concentration of antigen: 12 μg mL^{-1}; (d) Optimal concentration of antibody: 10 μg mL^{-1}.

ECL detection of Sudan I with the immunoassay

To evaluate the quantitative range and sensitivity of the mentioned immunosensor for Sudan I, the biosensor was characterized by quantifying different concentrations of standard solution Sudan I with Ab/Au/Cu as a signal probe. Figure 3 displays the ECL profiles of various concentrations of Sudan I in the range from 0.0005 to 100 ng mL^{-1}. It is obviously found that the ECL intensity of the biosensor is proportional to the logarithm of the Sudan I concentration with a linear regression equation of $y = 6760.9 + 1575.6\log C_{\text{Sudan I}}$ (ng mL^{-1}) and a regression coefficient of 0.996. Furthermore, the limit of detection was estimated to be 0.17 pg mL^{-1} according to 3SB/m (SB and m severally refer to standard deviation of the bland and slope of the linear regression equation), which is more sensitive than most of the previously reported methods (Table S1). The results

Table 1 Recoveries tests of Sudan I in the spiked real food samples (n = 3)

Sample	Added (ng mL^{-1})	Found (ng mL^{-1})	Intra-assay RSD (%)	Recovery (%)
Tomato sauce 1	0	N. D.[a]	–	–
Tomato sauce 2	0.001	0.00102 ± 0.00004	4.1	102
Tomato sauce 3	1	0.96 ± 0.05	5.4	96
Tomato sauce 4	100	114 ± 5	4.6	114
Chili sauce 1	0	N. D.[a]	–	–
Chili sauce 2	0.001	0.00099 ± 0.00006	5.8	99
Chili sauce 3	1	0.86 ± 0.01	1.3	86
Chili sauce 4	100	87 ± 5	6.1	87
Chili powder 1	0	N. D.[a]	–	–
Chili powder 2	0.001	0.00115 ± 0.00003	2.7	115
Chili powder 3	1	1.06 ± 0.02	1.9	106
Chili powder 4	100	101 ± 23	6.6	101

N. D.[a]: not detected

suggest that this immunosensor displays an extensive prospect of application.

Specificity, repeatability and stability of the immunosensor

The selectivity, stability and reproducibility as the important performances of a biosensor had been investigated meticulously and the results had been described in Fig. 4. Six different industrial dyes, including Sudan II, Sudan III, Sudan IV, Sunset Yellow, Lemon Yellow and Bright Blue at the concentrations of 10 ng mL^{-1} were performed with the method. The inset of Fig. 4a shows the structure of Sudan II, III, and IV that are highly similar to Sudan I, so the slight cross-reaction is acceptable. In contrast, the cross-reactivity of remaining three samples is negligible, indicated that the immunoassay has a favorable selectivity for detecting Sudan I.

Figure 4b depicts the ECL intensity of Sudan I target with 5 different concentrations upon continuous scanning for 5 cycles. A relatively stable ECL intensity was obtained and the relative standard deviation (RSD) was in the range of 1.3%~5.6%, indicating a satisfactory stability of the immunoassay. The intra- and inter-assays were used for estimating the reproducibility and precision of the biosensor. The measured RSD do not surpass 5%, which suggests that the reproducibility and precision of the ECL immunosensor are acceptable.

Application of real food samples analysis

To further demonstrate the practicability of the ECL biosensors for sample analysis, the assay were applied to three real-life samples under the optimized conditions. The contents of Sudan I in spiked samples were quantified according to the standard curve, which are summarized in Table 1. It is seen from Table 1 that the recoveries of the Sudan I from spiked samples are 86–115% with relative standard deviation (RSD) value in range of 1.3–6.6% ($n = 3$), revealing that this novel strategy is a feasible approach to detect Sudan I effectively in real food sample.

Conclusions

In summary, a novel competitive ECL immunosensor based on ECL-RET has been developed for the detection of Sudan I using Au/Cu NFs and Au-g-C_3N_4 NHs as the acceptor and donor, respectively. The composites used for the competition-type immunosensor have the following advantages: (1) Au/Cu nanoprobe provides a more uniform structure and a larger specific surface area for attaching antibodies; (2) Au NPs as an enhancer is chemically decorated onto the surface of g-C_3N_4 to form effective luminophore; (3) The well match between emission spectra of the donor and absorption spectra of acceptor makes the sensor exhibit excellent performance. The biosensor manifested remarkable sensitivity, reproducibility and precision, indicated that the competitive ECL immunosensor provide a convenient and reliable strategy for ultrasensitive detection of Sudan I. In case of replacing with the coating antigen and antibody for other analyte, the biosensor also can be applied to detect other small molecule.

Acknowledgements We really appreciate the support from the Science Fund from the National Natural Science Foundation of China (No.21175097, No. 31772053), the Project of Scientific and Technologic Infrastructure of Suzhou (SZS201207), the Project of State Key Laboratory of Analytical Chemistry for Life Science (SKLACLS1716), the Suzhou Industry (SYG201636), State and Local Joint Engineering Laboratory for Novel Functional Polymeric Materials and the Project Funded by the Priority Academic Program Development of Jiangsu Higher Education Institutions (No.YX10900212).

Compliance with ethical standards The author(s) declare that they have no competing interests.

References

1. Rebane R, Leito I, Yurchenko S, Herodes K (2010) A review of analytical techniques for determination of Sudan I–IV dyes in food matrixes. J Chromatogr A 1217:2747–2757
2. Rafii F, Hall JD, Cerniglia CE (1997) Mutagenicity of azo dyes used in foods, drugs and cosmetics before and after reduction by Clostridium species from the human intestinal tract. Food Chem Toxicol 35:897–901
3. Stiborova M, Martinek V, Rydlova H, Hodek P, Frei E (2002) Sudan I is a potential carcinogen for humans: evidence for its metabolic activation and Detoxication by human recombinant cytochrome P450 1A1 and liver Microsomes. Cancer Res 62:5678–5684
4. Møller P, Wallin H (2000) Genotoxic hazards of azo pigments and other colorants related to 1-phenylazo-2-hydroxynaphthalene. Mutat Res 462:13–30
5. Wang YZ, Yang H, Wang B, Deng AP (2011) A sensitive and selective direct competitive enzyme-linked immunosorbent assay for fast detection of Sudan I in food samples. J Sci Food Agric 91:1836–1842
6. He LM, Su YJ, Fang BH, Shen XG, Zeng ZL, Liu YH (2007) Determination of Sudan dye residues in eggs by liquid chromatography and gas chromatography–mass spectrometry. Anal Chim Acta 594:139–146
7. Ertaş E, Özer H, Alasalvar C (2007) A rapid HPLC method for determination of Sudan dyes and Para red in red chilli pepper. Food Chem 105:756–760
8. Cornet V, Govaert Y, Moens G, Loco JV, Egroodt JMD (2006) Development of a fast analytical method for the determination of Sudan dyes in chili- and curry-containing foodstuffs by high-performance liquid chromatography- photodiode array detection. Food Chem 54:639–644
9. Ling Y, Li JX, Qu F, Li NB, Luo HQ (2014) Rapid fluorescence assay for Sudan dyes using polyethyleneimine-coated copper nanoclusters. Microchim Acta 181:1069–1075
10. Zhang P, Li Z, Wang H, Zhuo Y, Yuan R, Chai YQ (2017) DNA nanomachine-based regenerated sensing platform: a novel electrochemiluminescence resonance energy transfer strategy for

ultra-high sensitive detection of microRNA from cancer cells. Nanoscale 9:2310–2316

11. Jiang XY, Wang HJ, Wang HJ, Zhuo Y, Yuan R, Chai YQ (2016) Self-enhanced N-(aminobutyl)-N-(ethylisoluminol) derivative-based electrochemiluminescence immunosensor for sensitive laminin detection using PdIr cubes as a mimic peroxidise. Nanoscale 8: 8017–8023
12. Dong YQ, Wu H, Shang PX, Zeng XT, Chi YW (2015) Immobilizing water-soluble graphene quantum dots with gold nanoparticles for a low potential electrochemiluminescence immunosensor. Nanoscale 7:16366–16371
13. Ma MN, Zhang X, Zhuo Y, Chai YQ, Yuan R (2015) An amplified electrochemiluminescent aptasensor using Au nanoparticles capped by 3,4,9,10- perylene tetracarboxylic acid-thiosemicarbazide functionalized C_{60} nanocomposites as a signal enhancement tag. Nanoscale 7:2085–2092
14. Xu JJ, Jiang DP, Qin YL, Xia J, Jiang DC, Chen HY (2017) C_3N_4 Nanosheet modified microwell Array with enhanced Electrochemiluminescence for Total analysis of cholesterol at single cells. Anal Chem 89:2216–2220
15. Ou X, Tan XR, Liu XF, Lu QY, Chen SH, Wei SP (2015) A signal-on electrochemiluminescence biosensor for detecting con a using phenoxy dextran-graphite-like carbon nitride as signal probe. Biosens Bioelectron 70:89–97
16. Cheng CM, Huang Y, Tian XQ, Zheng BZ, Li Y, Yuan HY, Xiao D, Xie SP, Choi MMF (2012) Electrogenerated chemiluminescence behavior of graphite-like carbon nitride and its application in selective sensing Cu^{2+}. Anal Chem 84:4754–4759
17. Zuo FM, Jin L, Fu XM, Zhang H, Yuan R, Chen SH (2017) An electrochemiluminescent sensor for dopamine detection based on a dual-molecule recognition strategy and polyaniline quenching. Sensors Actuators B Chem 244:282–289
18. Cheng CM, Huang Y, Wang J, Zheng BZ, Yuan HY, Xiao D (2013) Anodic electrogenerated chemiluminescence behavior of graphite-like carbon nitride and its sensing for rutin. Anal Chem 85:2601–2605
19. Guo ZY, Wu L, Hu YF, Wang S, Li X (2017) Potential-resolved "in-electrode" type electrochemiluminescence immunoassay based on functionalized g-C_3N_4 nanosheet and Ru-NH_2 for simultaneous determination of dual targets. Biosens Bioelectron 95:27–33
20. Ge L, Han CC, Liu J, Li YF (2011) Enhanced visible light photocatalytic activity of novel polymeric g-C_3N_4 loaded with Ag nanoparticles. Appl Catal A 409:215–222
21. Wang Y, Yao J, Li HR, Su DS, Antonietti M (2011) Highly selective hydrogenation of phenol and derivatives over a Pd@carbon nitride catalyst in aqueous media. J Am Chem Soc 133:2362–2365
22. Ge L, Han CC (2012) Synthesis of MWNTs/g-C_3N_4 composite photocatalysts with efficient visible light photocatalytic hydrogen evolution activity. Appl Catal B 117:268–274
23. Chen LC, Zeng XT, Si P, Chen YM, Chi YW, Kim DH (2014) Gold nanoparticle-graphite-like C_3N_4 nanosheet nanohybrids used for electrochemiluminescent immunosensor. Anal Chem 86:4188–4195
24. Wu MS, Shi HW, Xu JJ, Chen HY (2011) CdS quantum dots/$Ru(bpy)_3^{2+}$ electrochemiluminescence resonance energy transfer system for sensitive cytosensing. Chem Commun 47: 7752–7754
25. Ma HM, Li XJ, Yan T, Li Y, Liu HY, Zhang Y, Wu D, Du B, Wei Q (2016) Sensitive insulin detection based on Electrogenerated Chemiluminescence resonance energy transfer between $Ru(bpy)_3^{2+}$ and au nanoparticle-doped β-Cyclodextrin-Pb (II) metal–organic framework. ACS Appl Mater Interfaces 8:10121–10127
26. Zhou Y, Zhuo Y, Liao N, Chai YQ, Yuan R (2014) Ultrasensitive immunoassay based on a pseudobienzyme amplifying system of choline oxidase and luminol-reduced Pt@Au hybrid nanoflowers. Chem Commun 50:14627–14630
27. Zhai QF, Xing HH, Zhang XW, Li J, Wang E (2017) Enhanced Electrochemiluminescence behavior of gold-silver bimetallic nanoclusters and its sensing application for mercury(II). Anal Chem 89:7788–7794
28. Zhu WJ, Wang C, Li XJ, Khan MS, Sun X, Ma H, Fan DW, Wei Q (2017) Zinc-doping enhanced cadmium sulfide electrochemiluminescence behavior based on Au-Cu alloy nanocrystals quenching for insulin detection. Biosens Bioelectron 97:115–121
29. Ghodselahi T, Vesaghi MA, Shafiekhani A, Baghizadeh A, Lameii M (2008) XPS study of the Cu@Cu_2O core-shell nanoparticles. Appl Surf Sci 255:2730–2734
30. Hu LY, Zheng J, Zhao K, Deng AP, Li JG (2018) An ultrasensitive electrochemiluminescent immunosensor based on graphene oxide coupled graphite-like carbon nitride and multiwalled carbon nanotubes-gold for the detection of diclofenac. Biosens Bioelectron 101:260–267
31. Feng QM, Shen YZ, Li MX, Zhang ZL, Zhao W, Xu JJ, Chen HY (2015) Dual-wavelength electrochemiluminescence ratiometry based on resonance energy transfer between Au nanoparticles functionalized g-C_3N_4 nanosheet and $Ru(bpy)_3^{2+}$ for microRNA detection. Anal Chem 88:937–944